



Share Your Innovations through JACS Directory

# Journal of Nanoscience and Technology

Visit Journal at <http://www.jacsdirectory.com/jnst>

## Preparation and Characterization of Transparent Conducting FTO Thin Films by Chemical Spray Pyrolysis Method

Ebitha Eqbal, E. Hilal Rahman, E.I. Anila\*

Optoelectronic and Nanomaterials' Research Laboratory, Department of Physics, Union Christian College, Aluva – 683 102, Kerala, India.

### ARTICLE DETAILS

#### Article history:

Received 13 October 2018

Accepted 25 November 2018

Available online 25 December 2018

#### Keywords:

Thin Film

Spray Pyrolysis

Orthorhombic

Chromaticity Coordinates

### ABSTRACT

Fluorine doped tin oxide (FTO) thin films were synthesized by chemical spray pyrolysis method on glass substrates for 10 at.%, 15 at.%, 20 at.% of fluorine doping concentrations. Their structural, optical and electrical properties were investigated. X-ray diffraction (XRD) study shows polycrystalline nature of the films with orthorhombic crystal structure. The grain size ( $D$ ) was observed in the range of 14 nm to 30 nm. The FESEM images of the FTO thin films reveals that the films have smooth and homogeneous surface morphology with thin granular grains distributed throughout the surface. EDX analysis confirms the presence of Sn, O and F elements in the prepared FTO thin films. Photoluminescence (PL) spectrum shows a broad emission which covers near band edge (NBE) as well as deep level emissions (DLE) in the region 380 nm and 620 nm. From the hall effect measurements, it was observed that all the films exhibit n-type conductivity. The sample grown with 10 at. % of fluorine showed the highest transmission percentage (80%) with high mobility and conductivity, which are basic requirements for a TCO.

### 1. Introduction

Transparent conductive oxides (TCOs) have become increasingly important in a large variety of applications due to demands for optically-transparent, conducting materials. Typically, these applications use electrode materials that have greater than 80% transmission in the visible region, and a band gap greater than 3.2 eV for the best performing TCOs. TCOs are widely used in various optoelectronic applications like low emission glass, electrodes, organic light emitting diodes, lithium batteries, gas sensors, heat reflectors, polymer based electronics, flat panel displays, solar cells etc. [1-5]. In the case of fluorine doped tin oxide thin films (FTO), fluorine (F) is doped into tin oxide where fluorine substitutes for  $O^{2-}$  and acts as an electron donor, resulting in an n-type degenerate semiconductor. FTO is an ideal candidate for applications requiring TCO due to its ability to adhere strongly to glass, resistance to physical abrasion, chemical stability, high optical visible transparency, and electrical conductivity. Various techniques such as electron beam evaporation [6], magnetron sputtering [7], chemical vapour deposition [8], sol-gel [9], pulsed laser deposition [10] and spray pyrolysis [11] etc., were used for the deposition of FTO thin films.

In the present study, we are reporting FTO thin film for 10 at.%, 15at.%, 20 at.% of fluorine doping using chemical spray pyrolysis method at 350 °C and their structural, optical, and electrical properties.

### 2. Experimental Methods

The FTO thin films were deposited on ultrasonically cleaned glass substrate. Dehydrate stannous chloride ( $SnCl_2 \cdot 2H_2O$ ) was used for making the precursor solution for FTO thin films. An amount of required grams of  $SnCl_2 \cdot 2H_2O$  dissolved in 5 mL of concentrated hydrochloric acid (HCl) was heated at 90 °C for 10 min. HCl was added to break down the polymer molecules that were formed when diluting with methanol. This mixture diluted by adding methanol served as starting solution and the diluted solution was made up to 50 mL. For fluorine doping, ammonium fluoride ( $NH_4F$ ) (99% purity, Merck) dissolved in doubly distilled water (50 mL) was added to the starting solution, so that fluorine doping was in the range of 10 at.%, 15 at.%, 20 at.%. The spray solutions were magnetically stirred

for 1 h before spraying on the substrate. The samples were produced at a substrate temperature of 350 °C.

The structural characterization of the FTO thin films were carried out using X-ray diffraction analysis (XRD) on a Rigaku D-Max Geigerflex X-ray diffractometer using  $CuK\alpha$  radiation source ( $\lambda=1.5418 \text{ \AA}$ ) for  $2\theta$  values between  $10^\circ$  and  $60^\circ$  at room temperature. The optical characterization of the FTO thin films were studied by using Shimadzu UV-Vis spectrophotometer model-UV 1800. The morphology and microstructure of the prepared films were studied by Scanning electron microscopy (SEM) using JEOL JSM 7600F field emission scanning electron microscope. Elemental characterization of prepared films was done by energy dispersive X-ray spectrometer (EDX) using OXFORD XMX N. Pholuminescence (PL) studies were carried out using Fluoromax-4 Spectrofluorometer. The thickness of the film is measured using Stylus Profilometer (Surfext SJ-301). The electrical characterization was done using Hall Effect method using ECOPIA HMS-5000 in Vander Pauw configuration.

### 3. Results and Discussion

#### 3.1 Structural Analysis

To determine the crystal structure of the FTO thin film, X-ray diffraction techniques have been employed. The XRD pattern of FTO thin films is shown in Fig. 1(a). The grown films have exhibited strong orientation along (112) plane and also other reflections are obtained from the planes (113), (021), (006), (024), (118) and (133) which are in agreement with the standard JCPDS file no:78-1063, having orthorhombic crystal structure.

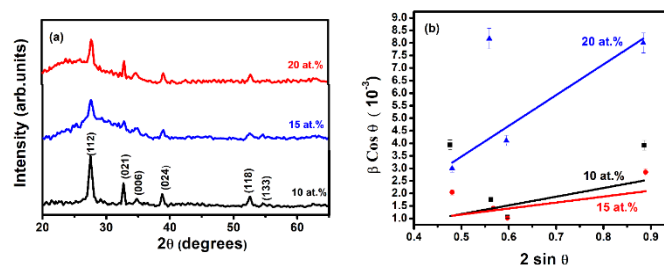


Fig. 1 (a) XRD pattern ,(b) W-H plot of FTO thin films

\*Corresponding Author: anilaei@gmail.com (E.I. Anila)

The average grain size of sprayed FTO thin film was calculated using the Scherrer’s formula [12].

$$D = \frac{0.9\lambda}{\beta \cos\theta} \tag{1}$$

where  $\lambda$  is the wavelength of X-ray radiations,  $\beta$  is the full width at half maximum of the peak corresponding to the diffraction peak, and  $\theta$  is the glancing angle. The average grain size evaluated from Scherrer’s formula for 10 at.%, 15 at.% and 20 at.% doping concentrations are 16.25 nm, 26.37 nm and 28.12 nm respectively. It was observed that the average grain size increases with increasing fluorine concentration. The dislocation density ( $\delta$ ) is used to determine the length of dislocation line per unit volume (lines/m<sup>2</sup>). Dislocation density values were calculated using the standard relations [13]

$$\text{Dislocation density } (\delta) = 1/D^2 \tag{2}$$

The dislocation density is tabulated in Table 1, and it was observed that the dislocation density decreases with increasing doping concentrations. The graph plotted by taking  $2\sin\theta$  along x-axis and  $\beta\cos\theta$  along y-axis is known as Williamson- Hall plot (W-H plot) shown in Fig. 1(b). The relation used for the calculation of lattice strain and crystallite size [12] is,

$$\beta \cos\theta = \frac{0.9\lambda}{D} + 2\xi \sin\theta \tag{3}$$

where  $\xi$  represents the lattice strain and  $\lambda$  is the wavelength of x- ray radiations,  $\beta$  is the full width at half maximum of the peak corresponding to the diffraction peak,  $\theta$  is the glancing angle and D is the grain size of the thin film. The average grain size evaluated from Scherrer’s formula and W-H plot of SnO<sub>2</sub> thin films for different doping concentrations are tabulated in Table 1. W-H plot for all the samples possess positive slope which is due to lattice elongation. The dislocation density is decreases with increasing fluorine doping concentration.

**Table 1** Grain size comparison data from Debye Scherrer’s formula and W-H plot

Fluorine doping level (at.%)	Grain size (D) from Scherrer’s formula (nm)	Dislocation density (x10 <sup>15</sup> ) (lines/ m <sup>2</sup> )	Grain size (D) from W-H plot (nm)	Lattice Strain
10	16.25	3.78	14.64	3.46
15	26.37	1.43	27.11	2.38
20	28.12	1.26	29.77	2.25

The reflection intensity for each peak contains information about the preferential or random growth of polycrystalline thin films, which is investigated by calculating the texture coefficient TC(hkl) for the plane from the following equation: [14],

$$TC(hkl) = \frac{I(hkl)}{\frac{1}{N} \sum I(hkl)} \tag{4}$$

where TC(hkl) is the texture coefficient of the hkl plane, I(hkl) is the intensity of each plane and N is the number of reflections. Table 2 shows texture coefficient of each (hkl) plane. The deviation of the texture coefficient from the unity implies the preferred orientation of the growth. The larger of texture coefficient deviates from unity, the higher will be the preferred orientation of a film. From the Table 2, it is clear that (112) has high preferred orientation for all the three samples.

**Table 2** Texture coefficient of each (hkl) plane

(hkl)	TC of Sample 1 (10 at.%)	TC of Sample 2 (15 at.%)	TC of Sample 3 (20 at.%)
(112)	2.17	2.29	2.11
(021)	0.9288	0.9664	1.03
(024)	0.5443	0.4370	0.4822
(118)	0.3520	0.3064	0.3696

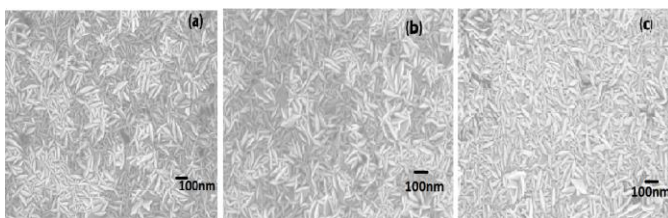


**Fig. 2** FESEM images of FTO thin films for (a) 10at.%, (b) 15 at.% (c) 20 at.% <https://doi.org/10.30799/jnst.176.18040529>

**3.2 Morphological Analysis**

The FESEM images of the FTO thin films for different molarities are shown in Fig. 2 which reveals that the films have smooth and homogeneous surface morphology with thin granular grains distributed throughout the surface.

**3.3 Elemental Analysis**

Elemental analysis of prepared FTO thin films was carried out by EDX. The Fig. 3 represents the EDX spectra of FTO thin films for different doping concentrations. EDX analysis confirms the presence of Sn, O and F elements in the prepared FTO thin films. There are small other peaks from the glass substrate was also observed.

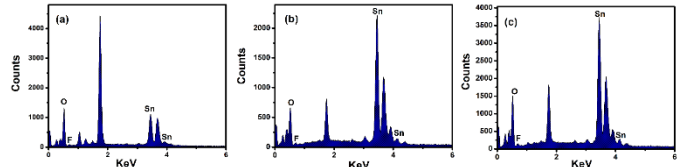


**Fig. 3** EDX Spectrum of FTO thin films for (a) 10 at.%, (b) 15 at.% (c) 20 at.%

**3.4 Optical Properties**

The variation of transmission percentage with respect to wavelength of FTO thin films for different fluorine doping levels is shown in Fig. 4(a). It was observed that the transmission percentage decreases with increasing doping concentration. The highest transmission percentage of 80% is observed for the sample deposited at 10 at.%. The optical band gap was examined using the relation proposed by Tauc, Davis and Mott [12].

$$\alpha h\nu = A(h\nu - E_g)^n \tag{5}$$

where  $h\nu$  is the photon energy,  $\alpha$  is the absorbance, A is the constant, n is ½ for direct transition. Fig. 4(b) shows the variation of  $(\alpha h\nu)^2$  and  $h\nu$  of FTO thin films. The optical band gap has then been determined by extrapolating the linear portion of the curve. The band gap of FTO thin films for 10 at.%, 15 at.% and 20 at.% is found to be 3.06 eV, 3.20 eV, and 2.80 eV respectively. Physically, the band gap effect in FTO system may originate from the change in nature and strength of the interaction potentials between the donors and host crystals. The decrease in band gap with doping level could be due to band tailing effect, whose primary cause is the presence of impurities and defects in the sample.

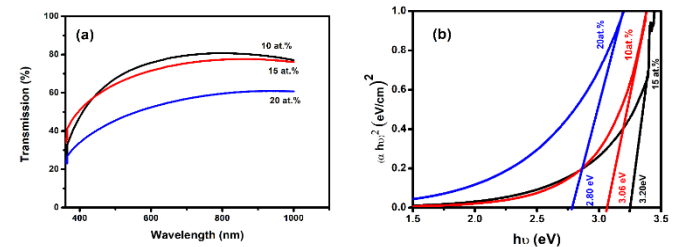


**Fig. 4** (a) Transmission spectrum and (b) Tauc Plot of FTO thin films

**3.5 Photoluminescence (PL) Studies**

The Fig. 5 shows the room temperature photoluminescence (PL) spectra collected by using an excitation wavelength of 320 nm.

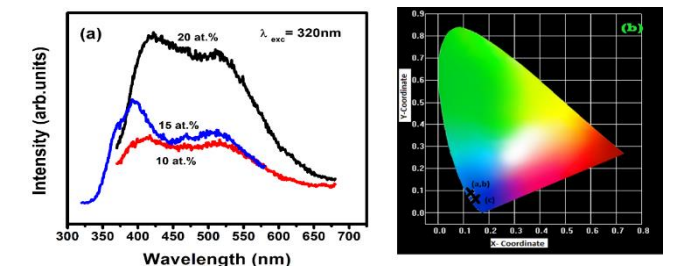


**Fig. 5** (a) PL spectra and (b) CIE diagram of FTO thin films for different doping concentrations

PL spectrum of the samples shows two broad emissions which covers near band edge (NBE) as well as deep level emissions (DLE) in the region 380 nm – 620 nm. NBE emission is generally due to excitons and DLE is due to intrinsic defects such as oxygen vacancies. From the Fig. 5, it was observed that the intensity of PL emission decreases with increasing

fluorine concentration. The broad peak at 380 nm corresponds to NBE emission and peak at 500 nm corresponds to the O-vacancy defect related DLE emission. The chromaticity coordinates (x,y) were calculated using the Commission Internationale de l'Eclairage (CIE) coordinate calculator from the emission spectrum. The color coordinates for FTO thin films in the CIE chromaticity diagram is shown in Fig. 5(b) by a solid cross (X). From the Fig. 5(b), it can be observed that all the three samples exhibit blue emission with CIE coordinates as x=0.128, y= 0.089; x=0.132, y=0.078; and x= 0.139, y=0.064 respectively for 10 at.%, 15 at.% and 20 at.% of fluorine doping. Hence these samples can be used for blue light emitting diodes (LEDs).

### 3.6 Electrical Studies

The FTO films exhibited n-type conduction with the mobility, whole concentration, and the resistivity values as shown in Table 2. It was observed that the conductivity decreases with increasing doping concentration. The conductivity and mobility was observed to be maximum for 10 at.% of fluorine doping. For 15 at.% fluorine doping, mobility decreases with doping because of carrier concentration is maximum for this doping percentage. Fig. 6 shows resistivity ( $\rho$ ), mobility ( $\mu$ ) and carrier concentration ( $n$ ) of FTO thin films as a function of the doping levels. For higher concentration of F in the solution, the resistivity increases due to the cancellation of the effect of oxygen vacancies by the substitution of fluorine atoms and also due to the accumulation of fluorine atoms at the grain boundaries creating Sn–F bonds. Because of that the conductivity decreases as doping concentration increases [15]. The presence of various defects in between valence band and conduction band are another reason for decreasing the conductivity of the samples. The optical studies, photoluminescent studies and high temperature electrical studies also confirms the presence of defects in the samples.

**Table 2** Electrical studies of FTO thin films

Doping Level (at. %)	Carrier Concentration ( $/\text{cm}^3$ )	Conductivity (S/cm)	Mobility ( $\text{cm}^2/\text{V.s}$ )	Thickness ( $\mu\text{m}$ )	Avg.Hall coefficient ( $\text{cm}^3/\text{C}$ )	Conductivity Type
10	$7.68 \times 10^{19}$	3.98	0.32	1.64	$8.12 \times 10^{-2}$	n
15	$2.52 \times 10^{20}$	2.28	0.56	1.59	$2.47 \times 10^{-2}$	n
20	$7.67 \times 10^{19}$	1.83	0.14	2.25	$8.12 \times 10^{-2}$	n

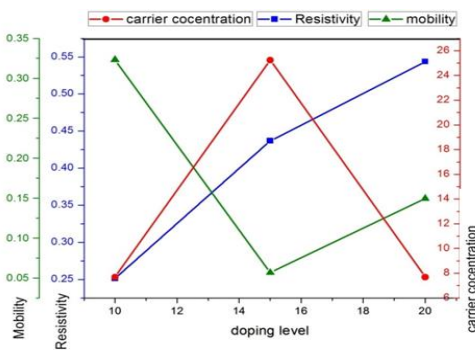


**Fig. 6** Variation of mobility, resistivity and carrier concentration as a function of fluorine doping level in  $\text{SnO}_2$  thin film

The variations in mobility as well as hall coefficient with doping concentration implies that the doping level of fluorine do influence the electrical properties of  $\text{SnO}_2$  thin film. Fig. 6 shows resistivity ( $\rho$ ), mobility ( $\mu$ ) and carrier concentration ( $n$ ) of FTO thin films as a function of the doping levels.

### 3.7 High Temperature Electrical Conductivity Studies

In order to study the mechanisms of conductivity, it is convenient to plot logarithm of the conductivity ( $\ln\sigma$ ) as a function of  $1000/T$ . Fig. 7(a-c) shows the relation between of  $\ln\sigma$  versus  $1000/T$  for FTO thin films for different doping concentrations in the range 308–423 K. The activation energy can be determined from the slopes of the Arrhenius plot. The activation energy  $E_a$  was calculated by applying the conductivity relation [24].

$$\sigma = \sigma_0 \exp\left(\frac{-E_a}{KT}\right) \quad (6)$$

where,  $\sigma$  is the conductivity, is a constant,  $k$  is Boltzmann constant and  $T$  is the temperature. The activation energy can be determined from the slopes of the Arrhenius plot. From the Fig. 7, it was observed that, all the samples show a semiconducting behavior. From Fig. 7(a), for sample 1, the activation energy is observed to be  $E_a = 0.07255$  eV. There is only one

activation energy observed for the first sample with least activation energy, for minimum activation energy the reaction will be more as compared to maximum activation energy. The conductivity is obtained maximum for this sample. From the Fig. 7(b), for sample 2, there is two activation energies observed with  $E_{a1} = 0.0863$  eV and  $E_{a2} = 0.07743$  eV. From Fig. 7(c), for sample 3, there is two activation energies observed with  $E_{a1} = 0.2424$  eV and  $E_{a2} = 0.09495$  eV. The reason for two activation energy observed for sample 2 and 3 is due to the presence of defect levels present in between the valence band and the conduction band.

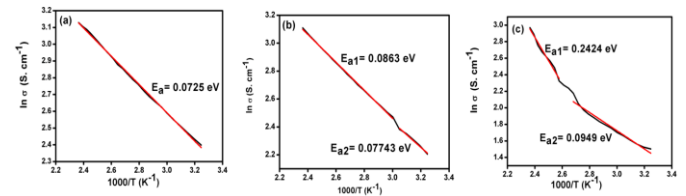


**Fig. 7** Arrhenius plot of FTO thin films for (a) 10 at.%, (b) 15 at.% and (c) 20 at.%

## 4. Conclusion

Polycrystalline, n-type FTO thin films with different fluorine doping concentrations were prepared by chemical spray pyrolysis method at 350 °C on glass substrates. XRD studies reveals that the films grown are of orthorhombic crystal structure. The grain size ( $D$ ) was observed in the range of 14 nm to 30 nm. The sample grown with 10 at.% fluorine showed the highest transmittance, mobility and conductivity, which are the basic requirements for a TCO. We can improve the conductivity of FTO thin films by increasing the substrate temperature and can be used for electrode applications.

## Acknowledgements

Authors thank Board of Research in Nuclear Sciences (BRNS), Department of Atomic Energy (DAE) for supporting this work through project 34/14/58/2014-BRNS.

## References

- [1] M. Oshima, K. Yoshino, Electron scattering mechanism of FTO films grown by spray pyrolysis method, *J. Electron. Mater.* 39(6) (2010) 819-822.
- [2] A.V. Moholkar, S. M. Pawar, K.Y. Rajpure, C.H. Bhosale, J.H. Kim, Effect of fluorine doping on highly transparent conductive spray deposited nanocrystalline tin oxide thin films, *Appl. Surf. Sci.* 255(23) (2009)9358-9364.
- [3] J. Ouerfelli, S.O. Djobo, J.C. Bernede, L. Cattin, M. Morsli, Y. Berredjem, Organic light emitting diodes using fluorine doped tin oxide thin films deposited by chemical spray pyrolysis as anode, *Mater. Chem. Phys.* 112(1) (2008) 198-201.
- [4] A. Smith, J.M. Laurent, D.S. Smith, J.P. Bonnet, R.R. Clemente, Relation between solution chemistry and morphology of  $\text{SnO}_2$ -based thin films deposited by a pyrolysis process, *Thin Solid Films* 266(1) (1995) 20-30.
- [5] A.A. Firooz, A.R. Mahjoub, A.A. Khodadadi, Highly sensitive CO and ethanol nanoflower-like  $\text{SnO}_2$  sensor among various morphologies obtained by using single and mixed ionic surfactant templates, *Sens. Actuators B: Chem.* 141(1) (2009) 89-96.
- [6] V. Senthilkumar, P. Vickraman, Structural, optical and electrical studies on nanocrystalline tin oxide ( $\text{SnO}_2$ ) thin films by electron beam evaporation technique, *J. Mater. Sci. Mater. Electron.* 21(6) (2010) 578-583.
- [7] Z.Y. Banyamin, P.J. Kelly, H. West, J. Boardman, Electrical and optical properties of fluorine doped tin oxide thin films prepared by magnetron sputtering, *Coatings* 4(4) (2014) 732-746.
- [8] H. Zhao, Q. Liu, Y. Cai, F. Zhang, Effects of water on the structure and properties of F-doped  $\text{SnO}_2$  films, *Mater. Lett.* 62(8-9) (2008) 1294-1296.
- [9] O.K. Varghese, L.K. Malhotra, Studies of ambient dependent electrical behavior of nanocrystalline  $\text{SnO}_2$  thin films using impedance spectroscopy, *J. Appl. Phys.* 87(10) (2000) 7457-7465.
- [10] H. Kim, R.C. Auyeung, A. Piqué, Transparent conducting F-doped  $\text{SnO}_2$  thin films grown by pulsed laser deposition, *Thin Solid Films* 516(15) (2008) 5052-5056.
- [11] G. Muruganatham, K. Ravichandran, K. Saravanakumar, A.T. Ravichandran, B. Sakthivel, Effect of solvent volume on the physical properties of undoped and fluorine doped tin oxide films deposited using a low-cost spray technique, *Superlatt. Microstruct.* 50 (2011) 722-733.
- [12] E. Eqbal, E.I. Anila, Properties of transparent conducting tin monoxide ( $\text{SnO}$ ) thin films prepared by chemical spray pyrolysis method, *Physica B: Condens. Matter.* 528 (2018) 60-65.
- [13] K. Ravichandran, G. Muruganatham, B. Sakthivel, Highly conducting and crystalline doubly doped tin oxide films fabricated using a low-cost and simplified spray technique, *Physica B: Condens. Matter.* 404(21) (2009) 4299-4302.
- [14] C.E. Benouis, M. Benhaliliba, F. Yakuphanoglu, A.T. Silver, M.S. Aida, A.S. Juarez, Physical properties of ultrasonic sprayed nanosized indium doped  $\text{SnO}_2$  films, *Synth Met.* 161(15-16) (2011) 1509-1516.
- [15] E. Elangovan, K. Ramamurthi, A study on low cost-high conducting fluorine and antimony-doped tin oxide thin films, *Appl. Surf. Sci.* 249(1-4) (2005) 183-196.